Mathematical Statistician and Engineering Applications
ISSN: 2326-9865

Development of Electric Waste Gate Actuator using Planetary Gear and DC Motor for Turbocharger

Soo-Whang Baek [+]
Sangmyung University, Dept. of Human Intelligence and Robot Eng., 31 Sangmyungdae-gil, Dongnam-gu, Cheonan-si, Chungcheongnam-do, 31066, Korea
swbaek@smu.ac.kr

Article Info
Page Number: 515 – 526
Publication Issue:
Vol. 71 No. 3 (2022)

Abstract
Nowadays, due to high oil prices and global warming, the automotive industry is striving to develop automobiles with high fuel efficiency and EWGAs capable of controlling the valve opening degree are preferred. In this study, an electric waste gate actuator (EWGA) for a turbocharger, used to improve the performance of a vehicle powertrain system by applying a DC motor and planetary gear, was developed. To this end, to efficiently manage the turbocharger, the waste gate valve mounted on it was replaced with an EWGA from an on-off vacuum type valve. This EWGA has the advantage of regulating the amount of air introduced into the engine by controlling the amount of exhaust gas entering through the turbocharger using the valve lift of the actuator.
The proposed EWGA was driven by the rotation of a DC motor and was designed to amplify the output torque of the motor by using a planetary gear with a high gear ratio of 40:1. For the planetary gear, the load was distributed inside the gear train, and a two-stage planetary gear was used, considering the stress and safety factor. Finally, an optimal EWGA prototype was manufactured and the feasibility of the proposed design was verified by evaluating the amount of current for both the 1st and 2nd tooth stages.

Keywords: Electric Waste Gate, Actuator, Planetary Gear, Design, Turbocharger, Automotive.

Article History
Article Received: *12 January 2022*
Revised: *25 February 2022*
Accepted: *20 April 2022*
Publication: *09 June 2022*

1. Introduction

In today's era of high-priced oil and global warming, the importance of fuel efficiency is being emphasized frequently. Concrete steps are being taken to develop high fuel-efficiency vehicles, and these steps are legally regulated by governments in many countries (He et al., 2012; Chen, 2015; Chen et al., 2015). In addition, research is being conducted on electronic control technology to protect the environment, reduce the emission of exhaust gases, and

[+] Corresponding author. Tel.: +82-41-550-5543; fax: +82-41-550-5549.
E-mail address: swbaek@smu.ac.kr.

increase the output of internal combustion engines (Baek, 2018; Lee and Baek, 2020; Baek and Lee, 2020; Kim, 2022).

For the efficient control of the turbocharger, a waste gate valve type actuator has been developed. In the past, mechanical waste gate valves that simply opened and closed the valve using the vacuum pressure generated by the engine have been mainly used (Romagnoli and Martinez-Botas, 2011; Chiong et al., 2014; Ketata et al., 2020).

The electric waste gate actuator serves to limit the charging pressure to a certain value with an increase in the engine rotation speed. In addition, the opening degree of the waste gate valve can be set arbitrarily, so that the required amount of boost pressure can always be generated in the turbocharger. Therefore, to reduce fuel consumption, there is an increasing trend in using electricity to control the position of the valve by changing the angle (Lujan et al., 2015; Dimitriou et al., 2017; Serrano et al., 2017).

The design requirements of the electric waste gate actuator included an operating temperature of -40 to 150 °C. The actuator rotated 90° clockwise and counterclockwise based on the output stage, and a large force was required to satisfy the final gear ratio of 40:1. Replacing the existing mechanical waste gate valve resulted in many space constraints. Particularly, reducing the volume and weight of the actuator to match the trend of weight reduction and miniaturization was imperative to replacing the valve. Additionally, to obtain high mechanical strength and output torque, various gear train methods have been proposed (Xu et al., 2018; Pardhiv and Srinivas, 2019; Sedak and Rosić, 2021).

The currently used EWGA structure in the industry has a multi-stage configuration of a general spur gear type and has economical disadvantages due to its large volume and weight. Therefore, this study proposes a structure that can produce high torque in a limited space by applying a two-stage planetary gear using the generally used planetary method. The proposed method is advantageous in that the use of two-stage planetary gears increases the gear ratio in the same volume and reduces the mechanical stress by distributing the load within the gear train. To verify the performance of the proposed structure, gear specifications were calculated and selected according to the application conditions using a gear specialized design program, and an optimal design was developed based on the analysis results. Finally, a prototype for verifying the tooth shape of the two-stage planetary gear was manufactured and assembled with a DC motor to realize the EWGA. The amount of current for the 1st and 2nd tooth stages of the planetary gear was evaluated to experimentally verify whether the current load amount of each planetary gear met the specified design conditions.

2. EWGA

EWGA has a structure that uses an electric motor rather than a conventional waste gate valve (mechanical) type to adjust the opening and closing of the valve. Therefore, it is possible to open and close each position, overcoming the disadvantage of the conventional mechanical type. In addition, improving the responsiveness of the structure at a low RPM provides more precise control than the existing mechanical type does.

2.1. Structure of EWGA

Figure 1 shows the structure of EWGA, which includes a DC motor, motor housing, and the

1st and 2nd stage planet gears and carriers. Figure 2 shows the assembly of the EWGA, composed of the DC motor and planetary gear. It is a type wherein the torque of the motor is taken as an input and the amplified output torque is generated from the link device through the gear train.

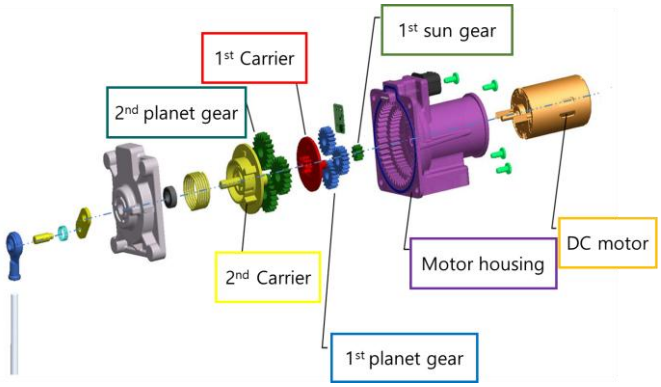

Fig. 1: Structure of the EWGA

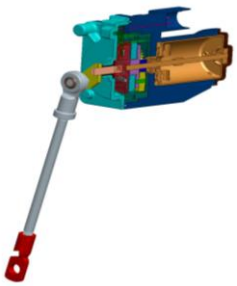

Fig. 2: Assembly of the EWGA

2.2. Characteristics of planetary gears

A planetary gear refers to a gear train that is based on a structure that rotates by supporting the planet gear around the sun gear with a carrier. A planetary gear is generally called a planetary device because its structure is similar to that of the solar system that combines rotation and orbital motion around the sun. It is also called an epicyclic gear, referring to the curve drawn by a point of the planetary gear that rotates and revolves around the sun gear. The planetary gear structure is spatially advantageous because the input and output shafts can be concentric. Therefore, the efficiency is increased because the friction loss is small due to the decrease in the transmission load and speed that each gear is responsible for. Planetary gears have a very high power transmission ratio per unit volume, so they can transmit several times more power than general gear reducers of the same size. Therefore, in this study, a structure wherein the final gear ratio is outputted as the product of the gear ratios in the first and second stages is proposed, and diagram of this two-stage planetary gear is shown in Fig. 3.

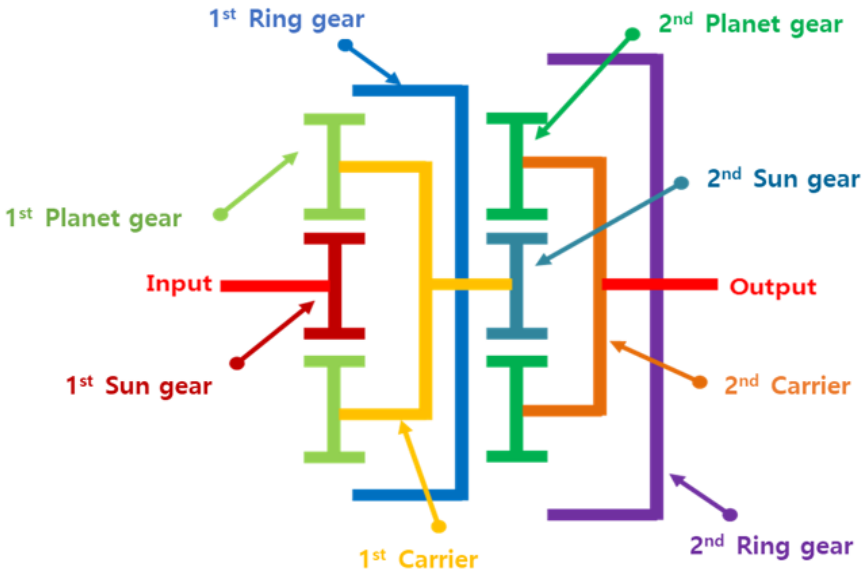

Fig. 3: Diagram of two-stage planetary gear

3. Design of EWGA planetary gear

EWGA requires precise control for maintaining flow control and high torque and providing quick responses to optimize the efficiency of the turbocharger system. Table 1 shows the EWGA requirements. In this study, we aim for a compact and lightweight design that satisfied these requirements. Therefore, we used the two-stage planetary gear structure in designing the structure of the gear train; the gear design process that was performed is shown in Fig. 4.

Table 1: Requirements of the EWGA

Items	**Descriptions**
Operating voltage	9~16 V
Current	Less than 1 A
Maximum driving force	More than 150 N
On/off response	Less than 150 ms
Operating temperature	-40℃ ~ +150 ℃ (Ambient)

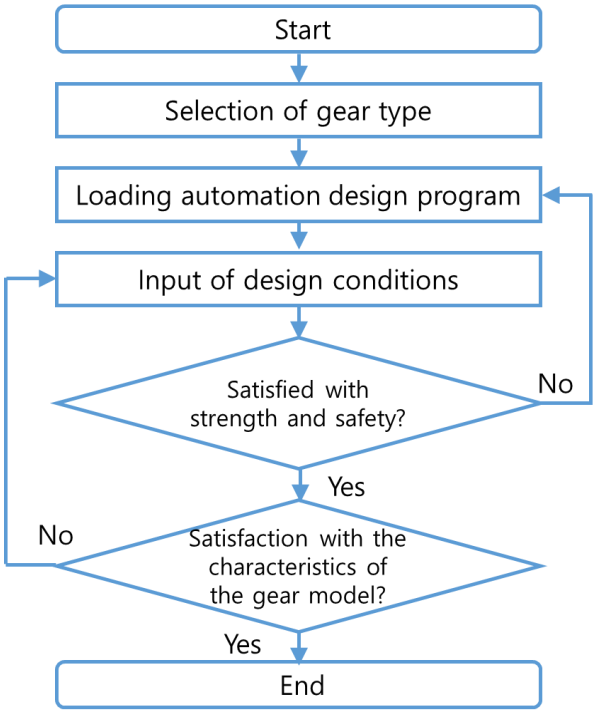

Fig. 4: The process of gear design

Each item in the design can be fine-sized and prioritized, considering the range of the gear ratio and tooth thickness to be obtained within the limited design space. The ISO/DIN standard has specified pressure angles of 14.5 and 20°; recently, 20° was specified. For heavy gears that require high strength, a larger pressure angle is usually used. In this study, the model was constructed by selecting the initial selection factors for gear design based on the module, engagement rate, and pressure angle. In Fig. 5, based on the pressure angle for each color, the X-axis represents the contact ratio and the Y-axis represents the normal module value. The model was selected to have a high contact ratio for the normal module to satisfy the specified conditions and to support parameter modifications for maintaining a small-size and lightweight design.

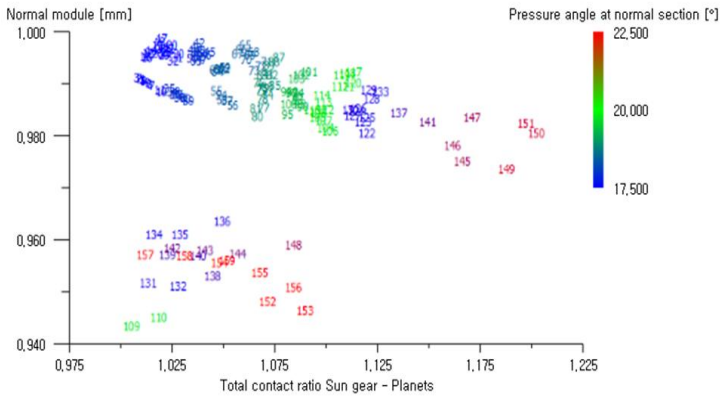

Fig. 5: Distribution of the pressure angle characteristics according to the contact ratio and module values

In this study, the following were considered when selecting the number of teeth in a planetary gear: 1) center distance, 2) gear sequential contact, 3) equal spacing, and 4) interference prevention.

First, the center distance condition is shown in Fig. 6. The relationship of $Z_p=(Z_r-Z_s)/2$ can be derived for the standard gear. In the case of a potential gear, $Z_p=(Z_r-Z_s-n)/2$, $n=1,2,3$ can be selected,

where Z_r is number of teeth of the ring gear, Z_s is number of teeth of the sun gear, Z_p is number of teeth of the planetary gear, N_p is the number of the planetary gears, and m is the module.

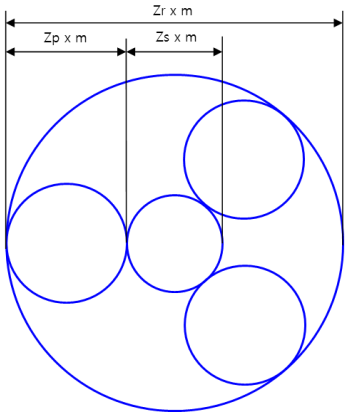

Fig. 6: Calculation of center distance

Second, gear sequential contact is advantageous when gears rotate in a sequentially meshed form. For example, if there is a sun gear with 5 teeth and a planetary gear with 10 teeth with a gear ratio of 2:1, only 2 specific teeth out of 10 are continuously meshed and rotated. However, in this case, uneven wear of the gear may occur, resulting in power transmission and noise. For the gears to contact sequentially, the ratios Z_p/Z_s and Z_r/Z_p should not become integers.

Third, to attain equally spaced arrangement, the number of teeth of the planetary gear should exist at regular intervals around the sun gear. For this, $(Z_s+Z_r)/N_p$ needs to have an integer value. For example, if N_p=3, planetary gears can be arranged at an equal spacing of 120°.

The fourth is the interference prevention condition, which is shown in Fig. 7. The planetary gear should not be large enough to interfere with the other neighboring gears. Interference does not occur when the center distance between the planetary gears is always larger than their outer diameter. Fig. 8 shows the numbers of the teeth selected for the planetary gear of the EWGA.

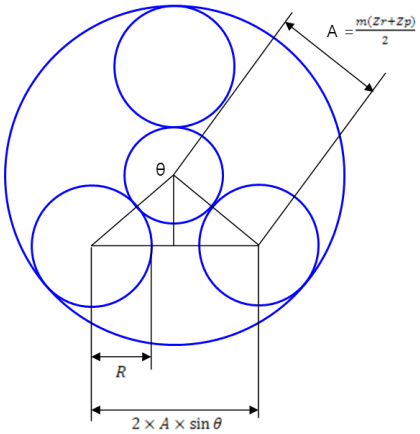

Fig. 7: Calculation of interference prevention

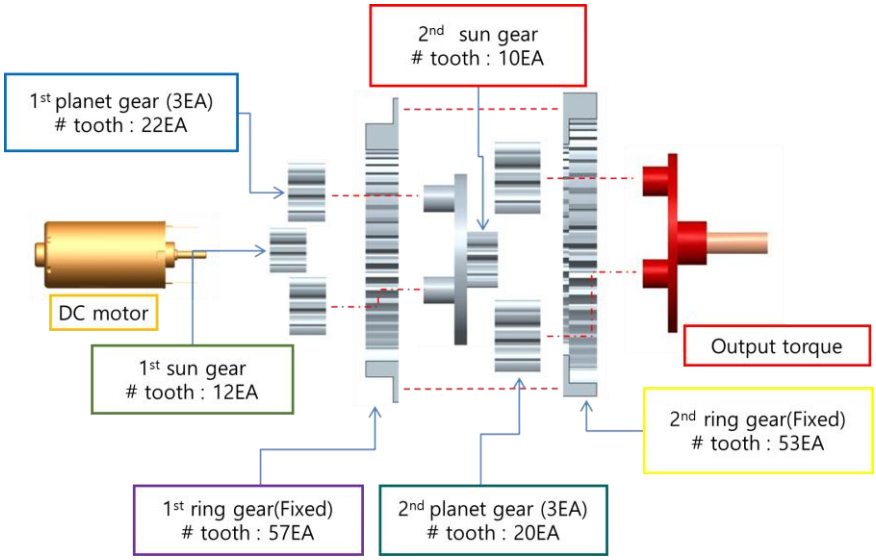

Fig. 8: Result of selection of number of teeth of planetary gear for EWGA

Table 2 shows the total contact ratio of the two-stage planetary gear designed according to the gear design process.

Table 2: Total contact ratio

Items	1st stage	2nd stage
Sun-planet	1.32	1.21
Planet-ring	1.80	1.30

To check the fatigue distribution in each stage, the sun gear and planetary gear were selected and the fatigue distribution was analyzed. As shown in Fig. 9, the inter-tooth stress at the tooth end was designed so that the involute curve did not intersect the tooth end. For the planetary gears used in this study, the 2nd stage gear showed higher stress values than the 1st stage gear did. As the gear ratio increased, the driving force appeared higher. As there were multiple stages, the driving force increased and the load was high.

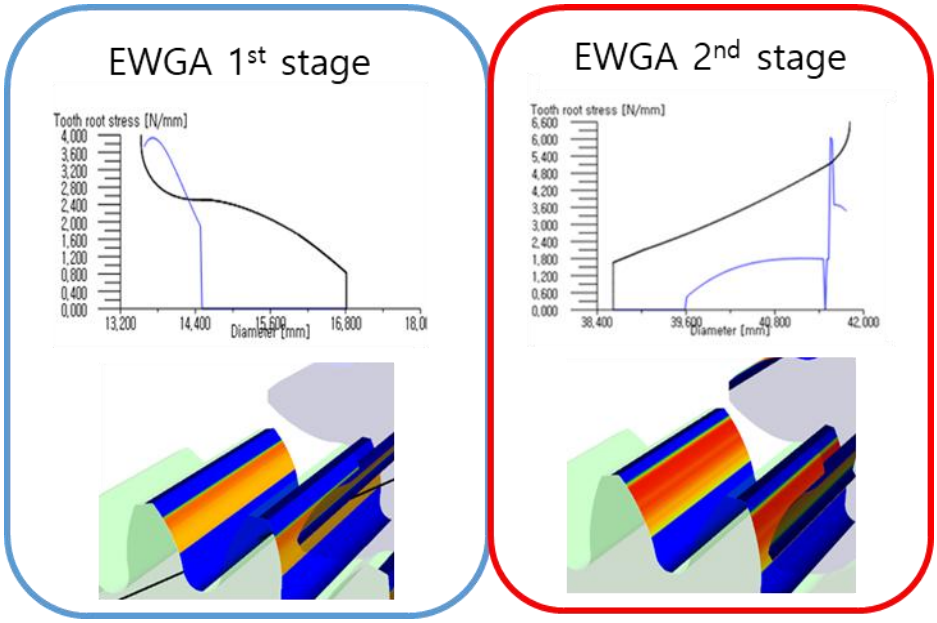

Fig. 9: Load distribution analysis of planetary gear teeth

Finally, the safety factor for the tensile strength was the value obtained by dividing the maximum bending stress by the allowable bending stress. The calculated values of the safety factor for the tooth strength of the 1st and 2nd stages are shown in Table 3. The safety factor of the gear was higher than that of the general spur gear, and it was verified that it had a good tooth strength design.

Table 3: Safety factors for the gears based on tooth strength

Items	Sun	Planet	Ring
1st stage	158.79	15.49	34.81
2nd stage	36.39	5.03	6.11

In addition, since three planetary gears were used in both the 1st and 2nd stages of the proposed tooth structure, the load was divided into three directions. Table 4 shows the load distribution ratio per the number of planetary gears.

Table 4: Load distribution ratios of planetary gears

Number of planetary gears	2	3	4	5
Load distribution ratio	0.58	0.41	0.38	0.27

4. Prototype production and experimental evaluation

To verify the optimality of the design in this study, a system driven by a DC motor was constructed by manufacturing a gear tooth type. Figure 10 shows a model extracted with a 3D CAD program based on the designed tooth type.

Fig. 10: 3D modeling for EWGA prototype

Prototypes were manufactured by using only the 1st stage and 2nd stage gear teeth. Since it was structurally difficult to measure the torque directly, a test was performed to compare the torque by applying power to the DC motor and measuring the current load. The 1st and 2nd stages were first operated separately and then operated simultaneously. The test composition of the prototype is as follows: 1) Only DC motor, 2) DC motor + 1 planetary gear, 3) DC motor + 2 planetary gears,
4) DC motor + 3 planetary gears, and 5) DC motor + 3 planetary gears + constraint condition (carrier).
Figure 11 shows the prototype of the EWGA used for the test along with the test environment. Figure 12 shows the current load for each EWGA prototype. A difference in the current load occurred when the free end was operated and there was a carrier on the planetary gear.

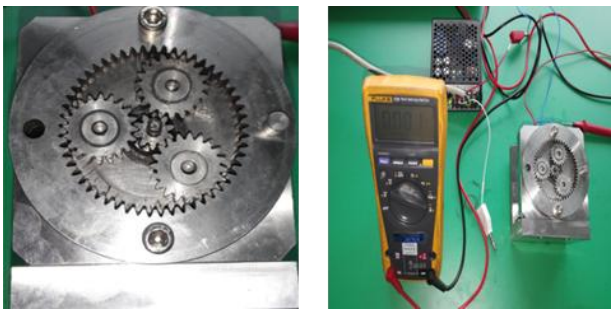

Fig. 11: Prototype of EWGA used for the test and the test environment

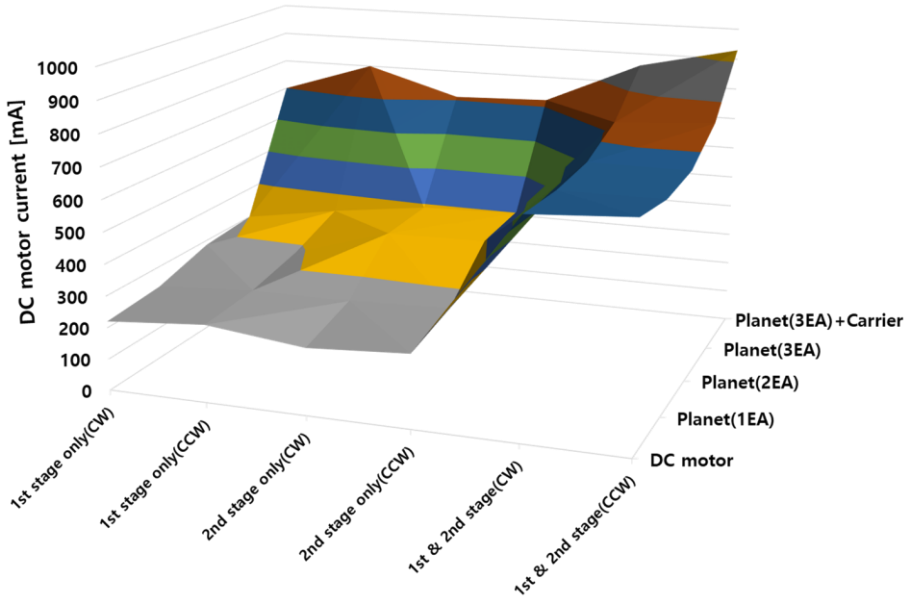

Fig. 12: Current load for each EWGA prototype

The measured currents for each EWGA prototype configuration are shown in Table 5. The difference in the values of the current loads according to the forward and reverse rotation conditions of the DC motor was assumed to be due to the difference in the loads in each open/close mode used for controlling the opening degree of the EWGA valve. The hole tolerance of each planetary gear and the shaft tolerance of the carrier had a large effect on the current loads. The mechanical operability of the EWGA was found satisfactory, considering the material composition of the gear.

Table 5: Current load of DC motor according to E-WGA prototype configuration

Items (motor direction)	DC motor	Planet (1EA)	Planet (2EA)	Planet (3EA)	Planet (3EA) +Carrier	Unit
1st stage only (CW)	220	235	285	300	700	mA
1st stage only (CCW)	245	255	290	350	800	mA
2nd stage only (CW)	210	255	385	390	710	mA
2nd stage only (CCW)	230	265	390	400	720	mA
1st & 2nd stage	670	660	670	730	860	mA

(CW)						
1st & 2nd stage (CCW)	690	660	670	750	930	mA

Through the current measurement experiment, it was possible to indirectly confirm the current characteristics consumed by the DC motor. It was confirmed that the DC motor current consumption of the EWGA applied with the planetary gear mentioned in the design target specification satisfied the condition of consuming only a current of 1A or less. Therefore, it was proved that applying the EWGA using the planetary difference of the method proposed in this study was possible. Additionally, the proposed EWGA can also be installed in an actual vehicle and verified under driving conditions wherein the turbocharger operates.

5. Conclusion

In this study, a planetary gear, one of the gear structures, was used and a two-stage planetary gear combined with two planetary gears was proposed to increase torque. As the load increased, the applicability of E-WGA was confirmed through a study to check the characteristics by applying a large module to the second gear and to perform an optimal design. In addition, the operability of the tooth type was confirmed by making an actual prototype. In this study, static calculation was applied. As a result of the test, the proposed EWGA driven by a dc motor satisfies the design requirements. In the future, it is considered that it is necessary to study the optimal tooth shape design by applying the material data considering the lifetime. Additionally, by changing the material of the planetary gear and the ring gear to a reinforced plastic material for vehicles, the optimal design is planned in consideration of the weight reduction of the EWGA.

6. Acknowledgements

This study was supported by the National Research Foundation of Korea (NRF) grant funded by the Korea government (MSIT) (No. 2021R1F1A1061567).

7. References

1. Baek, S.-W. (2018). Optimum shape design of a bldc motor for electric continuous variable valve timing system considering efficiency and torque characteristics. *Microsystem Technologies*, 24, 4441-4452. https://doi.org/10.1007/s00542-018-3991-2
2. Baek, S.-W. & Lee, S.W. (2020). Design optimization and experimental verification of permanent magnet synchronous motor used in electric compressors in electric vehicles. *Applied Sciences*, 10, 3235. https://doi.org/10.3390/app10093235
3. Chen, J.-S. (2015). Energy efficiency comparison between hydraulic hybrid and hybrid electric vehicles. *Energies*, 8, 4697-4723. https://doi.org/10.3390/en8064697

4. Chen, Z. Xiong, R. Wang, K. & Jiao, B. (2015). Optimal energy management strategy of a plug-in hybrid electric vehicle based on a particle swarm optimization algorithm. *Energies*, 8, 3661-3678. https://doi.org/10.3390/en8053661
5. Chiong, M. Rajoo, S. Romagnoli, A., Costall, A. & Martinez-Botasc, R. (2014). Integration of meanline and one-dimensional methods for prediction of pulsating performance of a turbocharger turbine. *Energy Conversion and Management*, 81, 270-281. https://doi.org/10.1016/j.enconman.2014.01.043
6. Dimitriou, P. Burke, R. Zhang, Q. Copeland, C. & Stoffels, H. (2017). Electric turbocharging for energy regeneration and increased efficiency at real driving conditions. *Applied Sciences*, 7, 350. https://doi.org/10.3390/app7040350
7. He, H. Liu, Z. Zhu, L. & Liu, X. (2012). Dynamic coordinated shifting control of automated mechanical transmissions without a clutch in a plug-in hybrid electric vehicle. *Energies*, 5, 3094-3109. https://doi.org/10.3390/en5083094
8. Ketata, A. Zied, D. & Mohamed, S. A. (2020). Impact of the wastegate opening on radial turbine performance under Steady and pulsating flow conditions. *Proceedings of the Institution of Mechanical Engineers, Part D: Journal of Automobile Engineering*, 234, 652-68. https://doi.org/10.1177/0954407019852494
9. Kim, K. (2022). A study on the application of Ferro-fluid to reduce no-load EMF THD for outer rotor motor. *Journal of Next-generation Convergence Technology Association*, 6, 157-162. https://doi.org/10.33097/JNCTA.2022.06.01.157
10. Lee, S.W. & Baek, S.-W. (2020). Implementation and experimental verification of smart junction box for low-voltage automotive electronics in electric vehicles. *Applied Sciences*, 10, 2214. https://doi.org/10.3390/app10072214
11. Lujan, J. Climent, H. & Rivas, M. (2015). Experimental characterization and modelling of a turbocharger gasoline engine compressor by-pass valve in transient operation. *SAE technical paper*, 2015-24-2524. https://doi.org/10.4271/2015-24-2524
12. Pardhiv, G. & Srinivas, P. (2019). Material selection for optimum design of planetary gear train used in automobile gear box. *International Journal for Modern Trends in Science and Technology*, 5, 48-59. http://dx.doi.org/10.2139/ssrn.3443710
13. Romagnoli, A. & Martinez-Botas, R. (2011). Performance prediction of a nozzled and nozzleless mixed-flow turbine in steady conditions. *International Journal of Mechanical Sciences*, 53, 557-574. https://doi.org/10.1016/j.ijmecsci.2011.05.003.
14. Sedak, M. & Rosić, B. (2021). Multi-objective optimization of planetary gearbox with adaptive hybrid particle swarm differential evolution algorithm. *Applied Sciences*, 11, 1107. https://doi.org/10.3390/app11031107
15. Serrano, J. Arnau, F. Andrés, T. & Samala, V. (2017). Experimental procedure for the characterization of turbocharger's waste-gate discharge coefficient. *Advances in Mechanical Engineering*, 9, 1-9. https://doi.org/10.1177/1687814017728242
16. Xu, Y. Ding, O. Qu, R. & Li, K. (2018). Hybrid multi-objective evolutionary algorithms based on decomposition for wireless sensor network coverage optimization. *Applied Soft Computing*, 68, 268-282. https://doi.org/10.1016/j.asoc.2018.03.053